

Synthesis, Characterization, Crystal Structure and Mass Transport Properties of Lanthanum β -Diketonate Glyme Complexes, Volatile Precursors for Metal–Organic Chemical Vapor Deposition Applications

Graziella Malandrino,[†] Cristiano Benelli,[‡] Francesco Castelli,[†] and Ignazio L. Fragala^{†,*}

Dipartimento di Scienze Chimiche, Università di Catania, V.le Andrea Doria 6, 95125 Catania, Italy, and Dipartimento di Chimica, Università di Firenze, Via Maragliano 77, 50144 Firenze, Italy

Received March 20, 1998. Revised Manuscript Received July 7, 1998

The monoglyme $\{\text{CH}_3\text{OCH}_2\text{CH}_2\text{OCH}_3\}$, diglyme $\{\text{CH}_3\text{O}(\text{CH}_2\text{CH}_2\text{O})_2\text{CH}_3\}$, and triglyme $\{\text{CH}_3\text{O}(\text{CH}_2\text{CH}_2\text{O})_3\text{CH}_3\}$ adducts of the lanthanum tris hexafluoroacetylacetoneato $\{\text{La(hfa)}_3\cdot\text{monoglyme}\cdot\text{H}_2\text{O}, \text{La(hfa)}_3\cdot\text{diglyme}$ and $\text{La(hfa)}_3\cdot\text{triglyme}\}$ have been synthesized in a single-step reaction. They have been characterized by elemental analyses, mass spectrometry, IR spectroscopy, ^1H and ^{13}C NMR spectroscopy. Single-crystal X-ray diffraction studies provide evidence of a mononuclear 9-coordinated complex with a monocapped square antiprismatic structure for the $\text{La(hfa)}_3\cdot\text{diglyme}$ (monoclinic system, space group = $P2_1/c$, $a = 10.075(2)$ Å, $b = 15.599(4)$ Å, $c = 21.038(9)$ Å, $\beta = 103.48(5)^\circ$, $Z = 4$). The $\text{La(hfa)}_3\cdot\text{monoglyme}\cdot\text{H}_2\text{O}$ consists of asymmetric units containing two similar molecules (monoclinic system, space group = $P2_1/c$, $a = 21.812(7)$ Å, $b = 13.232(3)$ Å, $c = 22.100(6)$ Å, $\beta = 111.28(4)^\circ$, $Z = 4$), while a more complex structure having asymmetric tetramolecular units has been found in the case of the $\text{La(hfa)}_3\cdot\text{triglyme}$ (monoclinic system, space group = $P2_1/n$, $a = 24.701(5)$ Å, $b = 11.762(4)$ Å, $c = 49.204(7)$ Å, $\beta = 104.32(3)^\circ$, $Z = 4$). The “thermal robustness” and mass transport properties of these adducts have been investigated by thermogravimetric analysis and chemical vapor deposition experiments. Thermal analysis data revealed the high volatility and very good thermal stability with a residue of less than 4% left. The $\text{La(hfa)}_3\cdot\text{diglyme}$ and $\text{La(hfa)}_3\cdot\text{triglyme}$ have been successfully applied to the low-pressure chemical vapor deposition (CVD) of LaAlO_3 and to the atmospheric-pressure CVD of lanthanum fluoride (LaF_3) films. The good quality of the deposited layers indicates that both the adducts are very attractive precursors for MOCVD applications.

Introduction

Particular attention has recently been devoted to the preparation of new lanthanide β -diketonate adducts with polyethers.^{1–4} Some of them exhibit improved properties, in terms of thermal stability and volatility, of potential interest for application as precursors in the MOCVD (metal–organic chemical vapor deposition) fabrication of electroceramics, e.g. superconductors such as $\text{LnBa}_2\text{Cu}_3\text{O}_{7-\delta}$,⁵ $\text{Pb}_2\text{Sr}_2\text{LnCu}_3\text{O}_{8-\delta}$,⁶ and $\text{La}_{2-x}\text{Sr}_x\text{CuO}_4$,⁷

piezoelectrics such as LaCuO_2 ,⁸ and buffer layers of LaAlO_3 .⁹ They may also find application in the synthesis of LaF_3 films, which act as a solid lubricant due to their lamellar hexagonal structure. Finally, they may be applied as precursors in the sol–gel technique since they are highly soluble in many organic solvents. Note that, in this context, the MOCVD technique offers a softer approach for all these applications, with lower processing temperatures and greater throwing power (versatility and adaptability) than alternative methodologies.¹⁰

To date, conventional lanthanide precursors, such as Ln(tmhd)_3 ($\text{H-tmhd} = 2,2,6,6\text{-tetramethyl-3,5-heptandione}$) have several drawbacks, essentially in the high quantity of residue left in commercial evaporators/bubblers and poor stability to the atmosphere.¹¹

- * E-mail: lfragala@dpchi.unicat.it.
- [†] Università di Catania.
- [‡] Università di Firenze.
- (1) Drake, S. R.; Lyons, A.; Otway, D. J.; Slawin, A. M. Z.; Williams, D. J. *J. Chem. Soc., Dalton Trans.* **1993**, 2379.
- (2) Drake, S. R.; Hursthouse, M. B.; Malik, K. M. A.; Miller, S. A.; Otway, D. J. *Inorg. Chem.* **1993**, 32, 4464.
- (3) Bradley, D. C.; Chudzynska, H.; Hursthouse, M. B.; Motellalli, M. *Polyhedron* **1994**, 13, 7.
- (4) Baxter, I.; Drake, S. R.; Hursthouse, M. B.; Abdul Malik, K. M.; McAleese, J.; Otway, D. J.; Plakatouras, J. C. *Inorg. Chem.* **1995**, 34, 1384.
- (5) a) Yang, K. N.; Dalichaouch, Y.; Ferreira, J. M.; Lee, B. W.; Neumeier, J. J.; Torikachvili, M. S.; Zhou, H.; Maple, M. B.; Hake, R. R. *Solid State Commun.* **1987**, 63, 515. b) Engler, E. M.; Lee, V. Y.; Nazzal, A. I.; Beyers, R. B.; Lim, G.; Grant, P. M.; Parkin, S. S. P.; Ramirez, M. L.; Vasquez, J. E.; Savoy, R. J. *J. Am. Chem. Soc.* **1987**, 109, 2848.

(6) Rouillon, T.; Hervieu, M.; Domengès, B.; Raveau, B. *J. Solid State Chem.* **1993**, 103, 63.

(7) Cava, R. J.; van Dover: R. B.; Batlogg, B.; Rietman, E. A. *Phys. Rev. Lett.* **1987**, 58, 408.

(8) Müller-Buschbaum, H. *Angew. Chem., Int. Ed. Engl.* **1989**, 28, 1472.

(9) Meng, X. F.; Pierce, F. S.; Wong, K. M.; Amos, R. S.; Xu, C. H.; Deaver, B. S., Jr.; Poon, S. J. *IEEE Trans. Magn.* **1991**, 27, 1638.

(10) Hitchman, M. L. and Jensen, K. F. *Chemical Vapor Deposition: Principles and Applications* Academic Press: London, 1993.

Table 1. Crystal Data and Experimental Parameters for Adducts 1–3

identification code	La(hfa) ₃ ·monoglyme·H ₂ O	La(hfa) ₃ ·diglyme	La(hfa) ₃ ·triglyme
empirical formula	LaC ₁₉ H ₁₅ O ₉ F ₁₈	LaC ₂₁ H ₁₇ O ₉ F ₁₈	LaC ₂₃ H ₂₁ O ₁₀ F ₁₈
formula weight	867.99	894.26	938.30
temperature, K	295(2)	293(2)	294(2)
wavelength, Å	0.71069	0.71069	0.71069
crystal system	monoclinic	monoclinic	monoclinic
space group	P2 ₁ /c	P2 ₁ /c	P2 ₁ /n
a, Å	21.812(7)	10.075(7)	24.701(5)
b, Å	13.232(3)	15.599(5)	11.762(4)
c, Å	22.100(6)	21.038(6)	49.204(7)
α , deg	90.00(1)	90.00(1)	90.00(1)
β , deg	111.28(4)	103.48(3)	104.32(3)
γ , deg	90.00(1)	90.00(1)	90.00(1)
volume, Å ³	5944(4)	3215(2)	13851(7)
Z	4	4	4
density (calcd), g/cm ³	1.936	1.847	1.800
absorption coefficient, mm ⁻¹	1.594	1.477	1.378
$F(0)$	3344	1736	7328
crystal size, mm	0.44 × 0.65 × 0.50	0.52 × 0.21 × 0.18	0.35 × 0.61 × 0.38
crystal color	colorless	colorless	colorless
θ range for data collection, deg	2.51–24.47	2.52–21.47	1.93–18.33
index ranges	−25 ≤ h ≤ 0, 0 ≤ k ≤ 15, −24 ≤ l ≤ 25	0 ≤ h ≤ 10, 0 ≤ k ≤ 16, −21 ≤ l ≤ 21	−8 ≤ h ≤ 20, −5 ≤ k ≤ 10, −43 ≤ l ≤ 42
no. of reflns measd	10134	3470	9511
independent reflections	9841 [R (int) = 0.0344]	3235 [R (int) = 0.0400]	9145 [R (int) = 0.0756]
refinement method		full-matrix least-squares on F^2	
data/restraints/parameters	9819/36/576	3235/0/366	9145/24/1762
goodness-of-fit on F^2	0.992	1.004	0.569
Final R indices [$I > 2\sigma(I)$]	$R_1 = 0.0594$, $wR_2 = 0.1511$	$R_1 = 0.0526$	$R_1 = 0.0835$
R indices (all data)	$R_1 = 0.0966$, $wR_2 = 0.1912$	$R_1 = 0.0599$	$R_1 = 0.0934$
largest diff peak and hole	1.140 and −0.798 e/Å ³	0.887 and −0.640 e/Å ³	0.852 and −1.042 e/Å ³
diff measurement devices		Enraf-Nonius CAD4	
weighting scheme		$w = 1/[\sigma^2(F_o)^2 + (0.1P)^2]$ where $P = (F_o^2 + 2F_c^2)/3$	
shift/esd mean value	0.009	0.002	0.016

In this scenario, novel monomeric, thermally stable, volatile, and water-free lanthanide complexes are of strategic relevance due to the lack of MOCVD precursors with suitable mass transport properties. This consideration prompted investigations on new, suitable, highly chelating molecular architectures which (i) inhibit oligomerization and water coordination processes and (ii) improve the thermal stability, volatility, and mass transport properties.

It is well-known that the combined use of fluorinated β -diketonates and of ancillary coordinated polyethers provides monomeric, volatile, and thermally stable alkaline-earth metal precursors.^{11–19} The same strategy has been applied to lanthanide ions and the tailoring of the molecular architecture of the ligand framework has yielded thermally stable, highly volatile, and very promising second-generation gadolinium²⁰ MOCVD precursors.

(11) Timmer, K.; Spee, K. I. M. A.; Mackor, A.; Meinenma, H. A.; Spek, A. L.; van der Sluis, P. *Inorg. Chim. Acta* **1991**, *190*, 109.

(12) Gardiner, R.; Brown, D. W.; Kirlin, P. S.; Rheingold, A. L. *Chem. Mater.* **1991**, *3*, 1053.

(13) Drake, S. R.; Miller, S. A. S.; Williams, D. J. *Inorg. Chem.* **1993**, *32*, 3227.

(14) Norman, J. A. T.; Pez, G. P. *J. Chem. Soc. Chem. Commun.* **1991**, 971.

(15) Thompson, S. C.; Cole-Hamilton, D. J.; Gilliland, D. D.; Hitchman, M. L.; Barnes, J. C. *Adv. Mater. Opt. Electron.* **1992**, *1*, 81.

(16) Malandrino, G.; Castelli, F.; Fragalà, I. L. *Inorg. Chim. Acta* **1994**, *224*, 203.

(17) Malandrino, G.; Fragalà, I. L.; Neumayer, D. A.; Stern, C. L.; Hinds, B. J.; Marks, T. J. *J. Mater. Chem.* **1994**, *4*, 1061.

(18) Nash, J. A. P.; Barnes, J. C.; Cole-Hamilton, D. J.; Richards, B. C.; Cook, S. L.; Hitchman, M. L. *Adv. Mater. Opt. Electron.* **1995**, *5*, 1.

(19) Neumayer, D. A.; Studebaker, D. B.; Hinds, B. J.; Stern, C. L.; Marks, T. J. *Chem. Mater.* **1994**, *6*, 878.

(20) Malandrino, G.; Incontro, O.; Castelli, F.; Fragalà, I. L.; Benelli, C. *Chem. Mater.* **1996**, *8*, 1292.

Herein, we report the synthesis and transport characteristics of three new lanthanum MOCVD precursors of general formula La(hfa)₃·L [H-hfa = 1,1,1,5,5,5-hexafluoroacetylacetone, L = CH₃O(CH₂CH₂O)_nCH₃ with n = 1, monoglyme (dimethoxyethane); n = 2, diglyme (bis(2-methoxyethyl)ether); and n = 3, triglyme (2,5,8,11-tetraoxadodecane)] and discuss their thermal stabilities and volatilities compared to first-generation lanthanum precursors. The effect of the polyether length on the thermal stability, volatility, and coordination sphere of the La(hfa)₃ moiety will be discussed as well.

Experimental Section

Reagents. Commercial La₂O₃, H-hfa, monoglyme, diglyme, and triglyme (Aldrich) were used without any further purification.

General Procedures. Elemental microanalyses were performed in the Analytical Laboratories of the University of Catania. ¹H NMR spectra were recorded on an FT Bruker 200 spectrometer. Infrared data were collected on a 684 Perkin-Elmer spectrometer either as Nujol or hexachlorobutadiene mulls between KBr plates. Thermal measurements were made using a Mettler 3000 system equipped with a TG 50 thermobalance, a TC 10 processor, and DSC 30 calorimeter. Weights of the samples were between 15 and 20 mg (TGA) and 4–10 mg (DSC). Analyses were made under prepurified nitrogen using a 5 °C/min heating rate. FAB mass spectra were obtained with a Kratos MS 50 spectrometer.

Synthesis of La(hfa)₃·Monoglyme·H₂O (1). La₂O₃ (2.441 g, 7.49 mmol) was first suspended in hexane (200 mL). Monoglyme (1.273 g, 14.13 mmol) was added to the suspension. H-hfa (8.821 g, 42.40 mmol) was added under vigorous stirring after 10 min and the mixture was refluxed under stirring for 1 h. The excess of lanthanum oxide was filtered off. White crystals precipitated after partial evaporation of the solvent. The colorless crystals were collected by filtration and dried

Table 2. Atomic Coordinates ($\times 10^4$) and Equivalent Isotropic Displacement Parameters ($\text{\AA}^2 \times 10^3$) for La(hfa)₃·Monoglyme·H₂O

atom	<i>x</i>	<i>y</i>	<i>z</i>	<i>U</i> (eq) ^a	atom	<i>x</i>	<i>y</i>	<i>z</i>	<i>U</i> (eq) ^a
La(1)	2412(1)	936(1)	4972(1)	40(1)	La(2)	2552(1)	1615(1)	77(1)	42(1)
O(1.1)	2098(3)	250(5)	5921(3)	61(2)	O(2.1)	2221(3)	523(5)	904(3)	56(2)
O(1.2)	1593(3)	2028(5)	5332(3)	57(2)	O(2.2)	1604(3)	2294(5)	409(3)	59(2)
C(1.1)	2534(5)	-447(9)	6380(5)	81(3)	C(2.1)	2661(5)	-214(8)	1311(5)	73(3)
C(1.2)	1768(5)	897(8)	6209(5)	68(3)	C(2.2)	1859(5)	1049(8)	1226(5)	69(3)
C(1.3)	1268(5)	1491(8)	5693(5)	71(3)	C(2.3)	1331(5)	1636(8)	746(5)	70(3)
C(1.4)	1179(5)	2761(8)	4909(5)	79(3)	C(2.4)	1126(6)	2985(9)	-11(6)	84(3)
O(1.3)	3005(3)	1993(4)	5961(3)	50(1)	O(2.3)	1533(3)	550(4)	-479(3)	52(1)
O(1.4)	3539(3)	249(5)	5602(3)	63(2)	O(2.4)	1881(3)	2280(5)	-1034(3)	60(2)
C(1.5)	3554(4)	1986(7)	6410(4)	51(2)	C(2.5)	1071(4)	560(6)	-1022(4)	47(2)
C(1.6)	4067(5)	1359(8)	6490(5)	71(3)	C(2.6)	982(5)	1185(8)	-1543(5)	63(2)
C(1.7)	4032(5)	533(9)	6079(5)	71(3)	C(2.7)	1416(5)	1963(7)	-1513(5)	58(2)
C(1.8)	3629(5)	2769(8)	6939(5)	69(3)	C(2.8)	549(4)	-234(7)	-1086(4)	61(2)
F(1.1)	3437(4)	3671(5)	6682(3)	94(2)	F(2.1)	234(3)	-22(5)	-687(4)	94(2)
F(1.2)	4241(3)	2887(6)	7352(3)	118(3)	F(2.2)	807(3)	-1144(4)	-905(4)	88(2)
F(1.3)	3260(4)	2532(6)	7271(3)	110(2)	F(2.3)	108(4)	-329(6)	-1666(3)	126(3)
C(1.9)	4637(7)	-67(13)	6184(9)	151(9)	C(2.9)	1307(6)	2545(10)	-2134(6)	93(4)
F(1.4)	5138(4)	169(11)	6682(8)	313(12)	F(2.4)	875(6)	2185(8)	-2649(4)	234(8)
F(1.5)	4568(7)	-1014(11)	6291(8)	248(10)	F(2.5)	1852(6)	2706(9)	-2226(4)	171(5)
F(1.6)	4774(6)	-182(14)	5666(9)	233(8)	F(2.6)	1119(6)	3475(7)	-2088(5)	167(5)
O(1.5)	1250(3)	356(4)	4385(3)	52(1)	O(2.5)	2753(3)	487(5)	-754(3)	56(2)
O(1.6)	1848(3)	1872(5)	3919(3)	58(2)	O(2.6)	3376(3)	2393(5)	-314(3)	63(2)
C(110)	818(4)	444(7)	3832(4)	48(2)	C(210)	3068(4)	588(7)	-1119(4)	55(2)
C(111)	853(5)	1049(7)	3340(5)	59(2)	C(211)	3494(5)	1343(8)	-1133(5)	65(2)
C(112)	1369(4)	1699(7)	3415(4)	53(2)	C(212)	3618(5)	2180(7)	-732(5)	60(2)
C(113)	1367(6)	2292(10)	2825(6)	86(3)	C(213)	2922(5)	-224(9)	-1642(5)	78(3)
F(1.7)	939(5)	2002(8)	2278(3)	187(6)	F(2.7)	2373(4)	-22(7)	-2123(4)	133(3)
F(1.8)	1215(6)	3242(7)	2872(5)	152(4)	F(2.8)	3340(4)	-301(8)	-1917(5)	153(4)
F(1.9)	1933(4)	2381(9)	2787(4)	159(4)	F(2.9)	2808(5)	-1098(5)	-1442(4)	138(3)
C(114)	213(5)	-187(7)	3725(4)	63(2)	C(214)	4133(5)	2916(9)	-755(5)	78(3)
F(110)	-256(4)	-56(7)	3165(4)	159(5)	F(210)	4423(5)	2707(7)	-1149(5)	148(4)
F(111)	349(3)	-1164(5)	3775(4)	100(2)	F(211)	4632(4)	2975(8)	-197(5)	150(4)
F(112)	-35(3)	-32(6)	4181(4)	106(2)	F(212)	3932(5)	3816(7)	-813(8)	225(8)
O(1.7)	3243(3)	2065(4)	4754(3)	51(1)	O(2.7)	3164(3)	2205(5)	1223(3)	55(2)
O(1.8)	2759(3)	175(5)	4123(3)	58(2)	O(2.8)	3621(3)	698(5)	612(3)	64(2)
C(115)	3591(4)	1974(6)	4410(4)	48(2)	C(215)	3714(4)	2066(7)	1655(4)	53(2)
C(116)	3562(5)	1227(7)	3967(5)	59(2)	C(216)	4208(5)	1467(8)	1634(5)	65(3)
C(117)	3133(4)	405(7)	3843(4)	49(2)	C(217)	4126(5)	845(8)	1106(5)	69(3)
C(118)	4107(5)	2777(8)	4524(5)	75(3)	C(218)	3822(5)	2656(8)	2269(5)	72(3)
F(113)	3942(4)	3642(5)	4693(4)	108(3)	F(213)	3350(4)	2512(7)	2492(3)	122(3)
F(114)	4635(4)	2543(7)	5044(6)	157(4)	F(214)	4387(4)	2487(8)	2739(3)	147(4)
F(115)	4354(6)	2854(7)	4086(5)	176(5)	F(215)	3800(4)	3642(6)	2160(4)	117(3)
C(119)	3105(5)	-286(8)	3284(5)	70(3)	C(219)	4705(7)	264(12)	1125(7)	117(5)
F(116)	3505(4)	-61(6)	2997(4)	120(3)	F(216)	4799(7)	257(17)	588(7)	274(10)
F(117)	2511(4)	-258(7)	2818(3)	114(3)	F(217)	4641(6)	-705(10)	1151(9)	250(9)
F(118)	3162(6)	-1221(6)	3467(4)	147(4)	F(218)	5239(4)	390(13)	1584(8)	300(11)
O(1.9)	2322(3)	-1048(5)	4888(3)	56(2)	O(2.9)	2618(3)	3594(5)	167(3)	55(2)

^a *U*(eq) is defined as ^a*U*(eq) is defined as one-third of the trace of the orthogonalized *U*_{ij} tensor.

Table 3. Selected Bond Lengths (Å) and Angles (deg) for One Molecule of the Asymmetric Unit of La(hfa)₃·Monoglyme·H₂O^a

Bond			
La(1)–O(1.1)	2.596(6)	La(1)–O(1.2)	2.636(6)
La(1)–O(1.3)	2.521(6)	La(1)–O(1.4)	2.513(6)
La(1)–O(1.5)	2.513(6)	La(1)–O(1.6)	2.526(6)
La(1)–O(1.7)	2.525(6)	La(1)–O(1.8)	2.477(6)
La(1)–O(1.9)	2.634(6)		
Angles			
O(1.8)–La(1)–O(1.5)	90.8(2)	O(1.8)–La(1)–O(1.4)	76.5(2)
O(1.5)–La(1)–O(1.4)	140.9(2)	O(1.8)–La(1)–O(1.3)	132.9(2)
O(1.5)–La(1)–O(1.3)	136.1(2)	O(1.4)–La(1)–O(1.3)	68.3(2)
O(1.8)–La(1)–O(1.7)	70.1(2)	O(1.5)–La(1)–O(1.7)	137.9(2)
O(1.4)–La(1)–O(1.7)	72.2(2)	O(1.3)–La(1)–O(1.7)	70.1(2)
O(1.8)–La(1)–O(1.6)	71.5(2)	O(1.5)–La(1)–O(1.6)	67.1(2)
O(1.4)–La(1)–O(1.6)	137.7(2)	O(1.3)–La(1)–O(1.6)	116.8(2)
O(1.7)–La(1)–O(1.6)	71.2(2)	O(1.8)–La(1)–O(1.1)	135.5(2)
O(1.5)–La(1)–O(1.1)	78.3(2)	O(1.4)–La(1)–O(1.1)	85.3(2)
O(1.3)–La(1)–O(1.1)	72.3(2)	O(1.7)–La(1)–O(1.1)	141.1(2)
O(1.6)–La(1)–O(1.1)	137.0(2)	O(1.8)–La(1)–O(1.9)	65.0(2)
O(1.5)–La(1)–O(1.9)	67.9(2)	O(1.4)–La(1)–O(1.9)	73.2(2)
O(1.3)–La(1)–O(1.9)	128.0(2)	O(1.7)–La(1)–O(1.9)	128.1(2)
O(1.6)–La(1)–O(1.9)	115.1(2)	O(1.1)–La(1)–O(1.9)	70.9(2)
O(1.8)–La(1)–O(1.2)	151.5(2)	O(1.5)–La(1)–O(1.2)	69.9(2)
O(1.4)–La(1)–O(1.2)	131.6(2)	O(1.3)–La(1)–O(1.2)	67.9(2)
O(1.7)–La(1)–O(1.2)	110.2(2)	O(1.6)–La(1)–O(1.2)	81.5(2)
O(1.1)–La(1)–O(1.2)	62.6(2)	O(1.9)–La(1)–O(1.2)	121.7(2)

^a Symmetry transformations used to generate equivalent atoms.

under vacuum. The yield was 86%. The melting point of the crude product was 60–64 °C. Anal. Calcd (Found) for

LaC₁₉H₁₅F₁₈O₉: C, 26.27 (26.20); H, 1.74 (1.86). The adduct quantitatively sublimes at 75–80 °C/10⁻³ mmHg. IR (Nujol or hexachlorobutadiene; ν , cm⁻¹): 3620 (w), 3540 (w), 2930 (vs), 1660 (vs), 1610 (w), 1570 (m), 1540 (m), 1495 (s), 1455 (s), 1380 (m), 1350 (vw), 1260 (s), 1200 (s), 1150 (s), 1100 (m), 1060 (s), 1030 (w), 1010 (vw), 950 (w), 860 (m), 805 (m), 770 (w), 740 (w), 660 (s). The NMR, MS, and IR data of the raw²¹ and sublimed adduct are identical.

Synthesis of La(hfa)₃·Diglyme (2). Compound **2** was prepared as described for the monoglyme adduct from 1.853 g (5.69 mmol) of La₂O₃, 6.311 g (30.34 mmol) of H-hfa, and 1.356 g (10.10 mmol) of diglyme to yield 91%. The melting point of the crude product was 74–76 °C. Anal. Calcd (Found) for LaC₂₁H₁₇F₁₈O₉: C, 28.19 (28.26); H, 1.91 (1.90). The adduct quantitatively sublimes at 65–70 °C/10⁻³ mmHg. IR (Nujol or hexachlorobutadiene; ν , cm⁻¹): 2930 (s), 1650 (vs), 1605 (w), 1555 (m), 1530 (m), 1495 (s), 1460 (s), 1380 (m), 1350 (w), 1260 (s), 1205 (s), 1140 (s), 1090 (s), 1065 (m), 1045 (s), 1010 (m), 945 (m), 870 (m), 835 (vw), 800 (m), 770 (w), 740 (m), 650 (s). The NMR, MS, and IR data of the raw and sublimed adduct are identical.

Synthesis of La(hfa)₃·Triglyme (3). Compound **3** was prepared as described for the monoglyme adduct from 1.939 g (5.94 mmol) of La₂O₃, 6.711 g (32.26 mmol) of H-hfa, and 1.917 g (10.75 mmol) of triglyme to yield 88%. Melting point of the crude product 88–90 °C.²² Anal. Calcd (Found) for LaC₂₃H₂₁F₁₈O₁₀: C, 29.42 (29.45); H, 2.26 (2.17). The adduct

(21) Used without any further purification.

Table 4. Atomic Coordinates ($\times 10^4$) and Equivalent Isotropic Displacement Parameters ($\text{\AA}^2 \times 10^3$) for La(hfa)₃·Diglyme

atom	<i>x</i>	<i>y</i>	<i>z</i>	<i>U</i> (eq) ^a
La(1)	9321(1)	1889(1)	1245(1)	49(1)
O(1)	7730(5)	1653(4)	138(3)	57(1)
O(2)	8564(6)	3262(4)	672(3)	66(2)
O(3)	11107(6)	2165(4)	641(3)	63(2)
O(4)	10810(6)	3085(3)	1770(3)	66(2)
O(5)	11413(6)	1242(4)	1996(3)	68(2)
O(6)	9197(6)	1863(3)	2405(3)	63(2)
O(7)	7603(6)	641(4)	1329(3)	68(2)
O(8)	9876(6)	355(4)	852(3)	72(2)
O(9)	6906(6)	2329(4)	1433(3)	69(2)
C(1)	6939(8)	2117(5)	-264(4)	55(2)
C(2)	6843(10)	2991(6)	-280(5)	65(2)
C(3)	7685(9)	3498(5)	193(4)	59(2)
C(4)	5980(10)	1634(7)	-800(5)	74(3)
F(1)	5632(9)	891(6)	-603(4)	166(4)
F(2)	6521(8)	1452(7)	-1280(4)	146(3)
F(3)	4823(8)	2005(5)	-1048(4)	140(3)
C(5)	7494(15)	4468(7)	123(6)	91(3)
F(4)	6699(13)	4726(5)	-402(5)	189(5)
F(5)	7111(18)	4794(6)	570(6)	244(8)
F(6)	8580(12)	4836(5)	114(9)	239(8)
C(6)	12046(8)	2694(6)	682(4)	58(2)
C(7)	12388(11)	3349(7)	1122(5)	76(3)
C(8)	11775(9)	3492(6)	1638(4)	63(2)
C(9)	12885(10)	2554(8)	195(5)	76(3)
F(07)	13537(18)	3177(8)	84(8)	290(11)
F(08)	13698(13)	1973(11)	326(5)	259(10)
F(09)	12241(8)	2332(8)	-374(4)	169(4)
C(10)	12293(16)	4205(9)	2119(7)	108(4)
F(10)	11348(12)	4685(6)	2221(6)	182(5)
F(11)	12846(15)	3911(7)	2683(5)	226(7)
F(12)	13175(12)	4698(7)	1950(6)	213(6)
C(11)	9955(9)	1701(5)	2954(4)	60(2)
C(12)	11257(9)	1380(6)	3099(5)	71(2)
C(13)	11894(9)	1184(6)	2598(4)	62(2)
C(14)	9278(12)	1881(8)	3523(5)	81(3)
F(13)	7993(7)	1675(6)	3391(3)	123(3)
F(14)	9851(8)	1472(6)	4070(3)	132(3)
F(15)	9344(9)	2688(6)	3671(4)	143(3)
C(15)	13337(12)	869(10)	2793(6)	98(4)
F(16)	13853(8)	741(9)	3385(4)	198(6)
F(17)	14139(10)	1296(14)	2585(8)	276(10)
F(18)	13515(14)	188(12)	2501(9)	284(11)
C(16)	11262(11)	120(8)	817(6)	95(3)
C(17)	9158(12)	-341(6)	1070(6)	89(3)
C(18)	7698(11)	-117(6)	955(6)	83(3)
C(19)	6209(10)	885(7)	1284(5)	82(3)
C(20)	6185(11)	1669(7)	1676(5)	82(3)
C(21)	6799(14)	3115(7)	1752(6)	93(4)

^a *U*(eq) is defined as one-third of the trace of the orthogonalized *U*_{ij} tensor.

quantitatively sublimes at 95–105 °C/10⁻³ mmHg. IR (Nujol or hexachlorobutadiene; ν , cm⁻¹): 2930 (s), 1660 (s), 1550 (s), 1525 (s), 1455 (s), 1370 (m), 1350 (m), 1245 (s), 1200(s), 1135 (s), 1080 (s), 1045 (s), 1020 (w), 1005 (w), 950 (w), 935 (w), 870 (m), 840 (m), 790 (m), 760 (w), 735 (w), 650 (m). The NMR, MS, and IR data of the raw and sublimed adduct are identical.

X-ray Structural Determination of Adducts 1–3. X-ray grade single crystals of **1–3** were grown from hexane. The colorless crystals, 0.44 × 0.65 × 0.50 mm for **1**, 0.52 × 0.21 × 0.18 mm for **2**, and 0.35 × 0.61 × 0.38 mm for **3**, were mounted on the tip of a quartz fiber. X-ray (Mo K α ; $\lambda = 0.71069$ Å) data were collected on an Enraf-Nonius CAD 4 four circle diffractometer. Unit cell parameters were derived from a least-squares refinements setting of 25 reflections in the 8 < θ < 16° range. They are reported in Table 1 with other experimental parameters. Corrections for Lorentz polarization and absorption (Ψ scan) were applied. The reflections were

Table 5. Selected Bond Lengths (Å) and Angles (deg) for La(hfa)₃·Diglyme

Bond Lengths			
La(1)–O(3)	2.471(6)	La(1)–O(6)	2.473(6)
La(1)–O(4)	2.485(6)	La(1)–O(2)	2.489(6)
La(1)–O(1)	2.527(5)	La(1)–O(5)	2.530(6)
La(1)–O(8)	2.634(6)	La(1)–O(7)	2.638(6)
La(1)–O(9)	2.645(6)		
Angles			
O(3)–La(1)–O(6)	136.1(2)	O(3)–La(1)–O(4)	70.2(2)
O(6)–La(1)–O(4)	74.8(2)	O(3)–La(1)–O(2)	77.2(2)
O(6)–La(1)–O(2)	114.3(2)	O(4)–La(1)–O(2)	69.8(2)
O(3)–La(1)–O(1)	86.1(2)	O(6)–La(1)–O(1)	137.7(2)
O(4)–La(1)–O(1)	134.9(2)	O(2)–La(1)–O(1)	67.8(2)
O(3)–La(1)–O(5)	77.9(2)	O(6)–La(1)–O(5)	66.7(2)
O(4)–La(1)–O(5)	72.1(2)	O(2)–La(1)–O(5)	139.7(2)
O(1)–La(1)–O(5)	140.7(2)	O(3)–La(1)–O(8)	76.3(2)
O(6)–La(1)–O(8)	111.0(2)	O(4)–La(1)–O(8)	132.1(2)
O(2)–La(1)–O(8)	133.9(2)	O(1)–La(1)–O(8)	73.4(2)
O(5)–La(1)–O(8)	68.1(2)	O(3)–La(1)–O(7)	137.0(2)
O(6)–La(1)–O(7)	74.7(2)	O(4)–La(1)–O(7)	149.5(2)
O(2)–La(1)–O(7)	122.4(2)	O(1)–La(1)–O(7)	70.7(2)
O(5)–La(1)–O(7)	97.4(2)	O(8)–La(1)–O(7)	62.7(2)
O(3)–La(1)–O(9)	146.8(2)	O(6)–La(1)–O(9)	66.2(2)
O(4)–La(1)–O(9)	102.7(2)	O(2)–La(1)–O(9)	70.1(2)
O(1)–La(1)–O(9)	76.6(2)	O(5)–La(1)–O(9)	132.2(2)
O(8)–La(1)–O(9)	123.6(2)	O(7)–La(1)–O(9)	62.7(2)

processed by the direct method program SIR 92²³ to determine the position of the La center and of the coordinated oxygen atoms. The other atomic parameters were determined by conventional Fourier difference syntheses and the whole set was refined by using the SHELXL93²⁴ package up to the final results listed in Tables 2–7. Anisotropic displacement parameters were introduced for all non-hydrogen atoms. The hydrogen atoms were included as idealized atoms riding on the respective carbon atoms with C–H bond lengths appropriate for the carbon atom hybridization. The isotropic displacement parameter of each hydrogen atom was fixed at 1.5 times the equivalent parameter of the carbon to which it is bound. The CF₃ groups were refined as rigid groups for all the structures. In some cases, difficulties were found in the refinement procedure due to the disorder present in the CF₃ groups of the hexafluoroacetylacetone moieties.

In the final stage of refinement, associated with data of adduct **1**, few peaks of intensity ranging between 1.14 and 0.98 e Å³ were observed close to some CF₃ groups. The refinement converged to a final agreement factor $R = 0.0594$ ($I > 2\sigma(I)$) and $R = 0.0966$ for all data.

For adduct **2**, the hydrogen atoms were added in calculated positions, and all the C–F bond distances were held fixed at 1.49 Å. The refinement converged to $R = 0.0526$ ($I > 2\sigma(I)$) and $R = 0.0599$.

For adduct **3**, the refinement converged to a final agreement factor $R = 0.0835$ ($I > 2\sigma(I)$) and $R = 0.0934$ for all data.

MOCVD Experiments. Atmospheric-pressure MOCVD depositions of LaF₃ films were performed under O₂ (80 sccm) flow, using a horizontal hot-wall reactor from the La(hfa)₃·diglyme source. Silicon (111) and glass substrates were used for the deposition of MF₃. The source temperature was controlled in the 160–170 °C range.

LaAlO₃ thin films were deposited under low-pressure in a horizontal hot-wall reactor from La(hfa)₃·diglyme and Al(acac)₃ (H-acac = acetylacetone) precursors. SrTiO₃ (100) and YSZ (100) were used as substrates in the 850–1050 °C range. Details of the MOCVD process have been reported elsewhere.²⁵

(23) Altomare, A.; Cascarano, G.; Giacovazzo, C.; Guagliardi, A. *J. Appl. Crystallogr.* **1994**, *27*, 1045.

(24) Sheldrick, G. M. SHELXL93, Program for Crystal Structure Determination, University of Göttingen: Göttingen, 1993.

(25) Malandrino, G.; Fragala, I. L.; Scardi, P. *Chem. Mater.* Submitted for publication.

(22) Obtained from comparison of DSC data and optical microscopy.

Table 6. Atomic Coordinates ($\times 10^4$) and Equivalent Isotropic Displacement Parameters ($\text{\AA}^2 \times 10^3$) for La(hfa)₃ Triglyme

atom	<i>x</i>	<i>y</i>	<i>z</i>	<i>U</i> (eq) ^a	atom	<i>x</i>	<i>y</i>	<i>z</i>	<i>U</i> (eq) ^a
La(01)	3701(1)	1585(1)	7840(1)	70	C(212)	4796(3)	6293(6)	8640(1)	117
O(1.1)	4595(2)	2578(3)	7730(1)	99	C(213)	4507(3)	9244(8)	9293(2)	213
O(1.2)	3988(2)	3745(3)	7994(1)	101	C(214)	6967(2)	5199(4)	10077(1)	92
O(1.3)	3087(1)	2732(3)	8115(1)	93	C(215)	7422(3)	5963(6)	10154(1)	112
O(1.4)	3311(2)	492(3)	8233(1)	102	C(216)	7457(2)	6829(5)	9976(1)	105
O(1.5)	4304(1)	1885(3)	8336(1)	88	C(217)	6982(2)	4177(5)	10275(1)	102
O(1.6)	4521(1)	253(3)	7968(1)	84	C(218)	7971(2)	7544(6)	10072(2)	151
O(1.7)	3790(1)	1085(3)	7366(1)	90	C(219)	6401(3)	9365(4)	9868(1)	115
O(1.8)	3471(2)	-461(3)	7722(1)	95	C(220)	6398(3)	9015(6)	10143(2)	130
O(1.9)	2673(1)	1198(3)	7631(1)	100	C(221)	6239(2)	7910(5)	10201(1)	101
O(1.10)	3303(1)	3070(3)	7490(1)	90	C(222)	6451(4)	10563(6)	9816(2)	178
C(1.1)	5010(3)	1949(6)	7628(1)	132	C(223)	6257(3)	7625(6)	10494(1)	120
C(1.2)	4790(2)	3664(5)	7839(1)	116	F(2.1)	4402(2)	6851(4)	8449(1)	160
C(1.3)	4311(2)	4383(5)	7845(1)	115	F(2.2)	4512(2)	5334(4)	8665(1)	172
C(1.4)	3522(3)	4443(5)	8045(1)	114	F(2.3)	5150(2)	5983(5)	8513(1)	194
C(1.5)	3275(3)	3816(5)	8241(1)	109	F(2.4)	4082(2)	9426(5)	9114(1)	273
C(1.6)	2747(3)	2068(6)	8253(1)	133	F(2.5)	4731(2)	9916(4)	9444(1)	290
C(1.7)	3080(3)	1175(7)	8423(1)	146	F(2.6)	4223(2)	8824(5)	9488(1)	271
C(1.8)	3594(3)	-444(5)	8373(1)	129	F(2.7)	7884(2)	8610(5)	10051(1)	209
C(1.9)	4752(2)	1511(4)	8472(1)	79	F(2.8)	8257(2)	7509(5)	9882(1)	224
C(1.10)	5112(2)	683(5)	8413(1)	100	F(2.9)	8314(2)	7374(6)	10291(1)	293
C(1.11)	4951(2)	86(5)	8163(1)	104	F(2.10)	7193(2)	3292(3)	10168(1)	158
C(1.12)	4954(3)	2162(7)	8750(1)	131	F(2.11)	7333(2)	4278(3)	10523(1)	135
C(1.13)	5363(4)	-845(6)	8107(2)	184	F(2.12)	6501(2)	3872(4)	10296(1)	171
C(1.14)	3755(3)	277(5)	7201(1)	130	F(2.13)	6278(3)	11244(4)	9947(2)	327
C(1.15)	3623(3)	-825(7)	7262(2)	152	F(2.14)	6507(4)	10913(5)	9611(1)	381
C(1.16)	3448(4)	-1127(4)	7527(1)	172	F(2.15)	6982(3)	10901(5)	9963(2)	290
C(1.17)	3871(3)	500(8)	6932(1)	201	F(2.16)	6417(3)	6595(5)	10564(1)	229
C(1.18)	3284(3)	-2366(6)	7572(1)	150	F(2.17)	6508(2)	8296(5)	10683(1)	207
C(1.19)	2314(3)	1602(6)	7422(1)	187	F(2.18)	5757(2)	7632(4)	10540(1)	193
C(1.20)	2379(3)	2479(7)	7230(2)	149	La(03)	8783(1)	2466(1)	9154(1)	76
C(1.21)	2902(3)	3117(5)	7284(1)	129	O(1.1)	8471(2)	1257(4)	9545(1)	113
C(1.22)	1793(3)	901(6)	7358(1)	121	O(3.2)	8134(2)	3400(3)	9455(1)	116
C(1.23)	2853(3)	4073(7)	7084(2)	139	O(3.3)	8975(2)	4639(4)	9357(1)	139
F(1.1)	4611(2)	2493(5)	8860(1)	208	O(3.4)	9597(2)	3669(4)	9029(1)	132
F(1.2)	5257(2)	3042(5)	8718(1)	210	O(3.5)	9653(2)	1217(3)	9220(1)	104
F(1.3)	5369(2)	1559(4)	8931(1)	179	O(3.6)	9458(1)	2636(3)	9628(1)	104
F(1.4)	5490(2)	-697(5)	7874(1)	207	O(3.7)	8332(2)	4009(3)	8833(1)	97
F(1.5)	5073(3)	-1815(4)	8057(2)	255	O(3.8)	7761(2)	2043(3)	8941(1)	108
F(1.6)	5750(2)	-1087(5)	8306(1)	241	O(3.9)	8573(2)	437(3)	9019(1)	104
F(1.7)	4392(1)	799(4)	6960(1)	142	O(3.10)	8828(2)	2064(3)	8671(1)	99
F(1.8)	3552(2)	1205(5)	6773(1)	208	C(3.1)	8783(3)	207(7)	9657(2)	172
F(1.9)	3814(2)	-343(5)	6775(1)	215	C(3.2)	8224(3)	1756(9)	9736(2)	184
F(1.10)	3483(3)	-2677(4)	7809(1)	227	C(3.3)	7857(3)	2576(8)	9605(2)	173
F(1.11)	3615(2)	-2930(5)	7446(1)	224	C(3.4)	8284(3)	4423(7)	9611(2)	163
F(1.12)	2838(2)	-2641(5)	7441(2)	249	C(3.5)	8489(3)	5157(7)	9433(2)	177
F(1.13)	1549(1)	1221(4)	7568(1)	139	C(3.6)	9272(3)	5381(6)	9210(2)	170
F(1.14)	1761(2)	-94(4)	7336(1)	202	C(3.7)	9755(3)	4807(8)	9173(2)	175
F(1.15)	1454(2)	1314(6)	7121(1)	229	C(3.8)	10028(3)	3195(10)	8906(2)	204
F(1.16)	2827(4)	3856(6)	6841(1)	324	C(3.9)	10092(2)	1053(5)	9405(1)	90
F(1.17)	2500(2)	4674(6)	7078(2)	386	C(3.10)	10263(2)	1513(5)	9669(1)	97
F(1.18)	3256(3)	4725(5)	7141(1)	276	C(3.11)	9915(2)	2262(5)	9754(1)	85
La(02)	6105(1)	6712(1)	9536(1)	75	C(3.12)	10456(3)	145(8)	9320(2)	152
O(2.1)	5237(2)	5591(3)	9650(1)	100	C(3.13)	10134(3)	2789(7)	10036(2)	136
O(2.2)	5883(2)	4544(3)	9350(1)	103	C(3.14)	8017(3)	3990(5)	8602(1)	149
O(2.3)	6746(2)	5683(3)	9243(1)	114	C(3.15)	7501(4)	3256(8)	8538(2)	177
O(2.4)	6445(2)	7876(4)	9145(1)	121	C(3.16)	7415(3)	2347(6)	8715(1)	219
O(2.5)	5453(1)	6464(3)	9052(1)	90	C(3.17)	7954(3)	5050(8)	8439(1)	150
O(2.6)	5282(1)	8000(3)	9448(1)	107	C(3.18)	6916(3)	1670(6)	8632(1)	120
O(2.7)	6557(1)	5191(3)	9867(1)	86	C(3.19)	8491(4)	-128(5)	8800(1)	203
O(2.8)	7126(1)	7125(3)	9756(1)	94	C(3.20)	8579(4)	313(14)	8539(2)	306
O(2.9)	6317(2)	8706(3)	9663(1)	105	C(3.21)	8783(4)	1372(8)	8473(2)	388
O(2.10)	6085(2)	7149(3)	10020(1)	91	C(3.22)	8484(5)	-1409(7)	8866(1)	320
C(2.1)	4753(2)	6141(7)	9720(1)	145	C(3.23)	8799(3)	1841(10)	8202(1)	191
C(2.2)	5062(2)	4514(5)	9511(1)	115	F(3.13)	8407(3)	2124(9)	8041(2)	471
C(2.3)	5569(3)	3908(5)	9503(1)	114	F(3.14)	8756(4)	803(8)	8076(1)	334
C(2.4)	6342(3)	3913(5)	9302(1)	122	F(3.15)	9296(2)	1846(7)	8204(1)	260
C(2.5)	6587(3)	4656(7)	9112(1)	157	F(3.1)	10200(2)	-702(5)	9206(1)	254
C(2.6)	7030(3)	6451(8)	9096(2)	178	F(3.2)	10691(2)	514(6)	9123(1)	262
C(2.7)	6687(3)	7328(9)	8954(2)	182	F(3.3)	10881(2)	-119(5)	9510(1)	245
C(2.8)	6167(4)	8927(7)	9024(2)	195	F(3.4)	9797(2)	2964(9)	10168(1)	351
C(2.9)	5004(2)	6859(5)	8913(1)	88	F(3.5)	10569(2)	2325(5)	10203(1)	197
C(2.10)	4673(2)	7709(5)	8985(1)	104	F(3.6)	10292(4)	3728(5)	10037(1)	337
C(2.11)	4873(2)	8238(6)	9251(1)	112	F(3.7)	6963(3)	561(5)	8618(1)	281

Table 6 (Continued)

atom	<i>x</i>	<i>y</i>	<i>z</i>	<i>U(eq)^a</i>	atom	<i>x</i>	<i>y</i>	<i>z</i>	<i>U(eq)^a</i>
F(3.8)	6603(2)	1774(5)	8796(1)	214	C(412)	10062(3)	7377(9)	7484(1)	184
F(3.9)	6623(3)	1738(6)	8374(1)	262	C(413)	11581(3)	4606(7)	7702(2)	180
F(310)	7613(2)	4930(4)	8176(1)	146	C(414)	11714(2)	4438(4)	8704(1)	113
F(311)	8407(2)	5389(6)	8423(1)	260	C(415)	12291(2)	4776(6)	8775(1)	121
F(312)	7744(3)	5832(4)	8548(1)	223	C(416)	12459(2)	5856(5)	8739(1)	116
F(316)	8649(6)	-1757(6)	9085(2)	427	C(417)	11608(3)	3203(8)	8716(2)	246
F(317)	8500(3)	-1937(5)	8651(2)	296	C(418)	13079(3)	6110(6)	8829(2)	128
F(318)	7964(3)	-1771(5)	8816(2)	290	C(419)	11882(2)	8675(5)	9005(1)	101
La(04)	11183(1)	7090(1)	8426(1)	75	C(420)	11757(2)	7967(6)	9219(1)	108
O(4.1)	10220(2)	5921(4)	8377(1)	118	C(421)	11363(2)	7096(5)	9156(1)	97
O(4.2)	10308(2)	8168(4)	8517(1)	124	C(422)	12306(4)	9528(6)	9094(1)	179
O(4.3)	10930(2)	9258(5)	8240(1)	135	C(423)	11209(3)	6463(6)	9388(1)	114
O(4.4)	11840(2)	8163(3)	8160(1)	110	F(4.1)	9619(2)	7482(8)	7534(1)	319
O(4.5)	10546(2)	7309(3)	7938(1)	102	F(4.2)	9980(3)	7092(7)	7235(1)	285
O(4.6)	11426(2)	5756(3)	8069(1)	101	F(4.3)	10136(3)	8418(6)	7434(1)	307
O(4.7)	11313(1)	5092(3)	8590(1)	104	F(4.4)	12084(2)	4861(5)	7737(1)	240
O(4.8)	12165(2)	6659(3)	8638(1)	114	F(4.5)	11598(2)	3683(4)	7862(1)	240
O(4.9)	11670(2)	8626(3)	8752(1)	97	F(4.6)	11394(2)	4271(4)	7458(1)	180
O(410)	11102(1)	6788(3)	8916(1)	92	F(4.7)	11937(2)	2514(4)	8737(2)	332
C(4.1)	10086(3)	4937(5)	8187(1)	145	F(4.8)	11505(3)	3070(5)	8985(1)	275
C(4.2)	9725(3)	6559(7)	8374(2)	151	F(4.9)	11145(3)	2856(5)	8641(2)	316
C(4.3)	9906(3)	7445(7)	8581(2)	167	F(410)	13270(2)	6370(5)	8620(1)	180
C(4.4)	10115(3)	9252(6)	8378(2)	152	F(411)	13384(2)	5248(5)	8950(1)	218
C(4.5)	10598(3)	9855(7)	8374(2)	161	F(412)	13206(2)	6877(4)	9014(1)	177
C(4.6)	11385(3)	9923(6)	8179(1)	161	F(413)	12514(2)	10043(5)	8942(1)	310
C(4.7)	11705(3)	9241(7)	8036(1)	151	F(414)	12105(3)	10420(4)	9179(2)	323
C(4.8)	12255(3)	7684(8)	8044(2)	156	F(415)	12652(2)	9382(4)	9324(1)	257
C(4.9)	10517(2)	6864(5)	7704(1)	100	F(416)	10680(1)	6630(4)	9384(1)	140
C(410)	10840(3)	6029(6)	7623(1)	113	F(417)	11286(2)	5361(4)	9374(1)	175
C(411)	11262(2)	5520(5)	7816(1)	96	F(418)	11525(2)	6722(5)	9640(1)	183

^a *U(eq)* is defined as one-third of the trace of the orthogonalized *U_{ij}* tensor.

Table 7. Selected Bond Lengths (Å) and Angles (deg) for One Molecule of the Asymmetric Unit of La(hfa)₃·Triglyme

Bonds			
La(01)–O(1.1)	2.670(4)	La(01)–O(1.6)	2.514(3)
La(01)–O(1.2)	2.696(4)	La(01)–O(1.7)	2.468(3)
La(01)–O(1.3)	2.641(4)	La(01)–O(1.8)	2.508(3)
La(01)–O(1.4)	2.692(4)	La(01)–O(1.9)	2.534(3)
La(01)–O(1.5)	2.549(3)	La(01)–O(110)	2.479(3)

Angles

O(1.7)–La(01)–O(110)	67.89(11)	O(1.7)–La(01)–O(1.8)	67.71(11)
O(110)–La(01)–O(1.8)	119.16(10)	O(1.7)–La(01)–O(1.6)	80.43(11)
O(110)–La(01)–O(1.6)	140.27(12)	O(1.8)–La(01)–O(1.6)	65.32(11)
O(1.7)–La(01)–O(1.9)	83.52(12)	O(110)–La(01)–O(1.9)	70.07(12)
O(1.8)–La(01)–O(1.9)	65.58(12)	O(1.6)–La(01)–O(1.9)	130.83(12)
O(1.7)–La(01)–O(1.5)	140.39(11)	O(110)–La(01)–O(1.5)	127.23(11)
O(1.8)–La(01)–O(1.5)	113.54(11)	O(1.6)–La(01)–O(1.5)	66.60(11)
O(1.9)–La(01)–O(1.5)	134.71(12)	O(1.7)–La(01)–O(1.3)	143.44(10)
O(110)–La(01)–O(1.3)	79.48(12)	O(1.8)–La(01)–O(1.3)	118.85(12)
O(1.6)–La(01)–O(1.3)	136.01(10)	O(1.9)–La(01)–O(1.3)	69.82(11)
O(1.5)–La(01)–O(1.3)	73.28(10)	O(1.7)–La(01)–O(1.1)	69.00(11)
O(110)–La(01)–O(1.1)	75.91(11)	O(1.8)–La(01)–O(1.1)	121.66(12)
O(1.6)–La(01)–O(1.1)	70.60(11)	O(1.9)–La(01)–O(1.1)	142.41(11)
O(1.5)–La(01)–O(1.1)	79.42(11)	O(1.3)–La(01)–O(1.1)	119.31(12)
O(1.7)–La(01)–O(1.4)	134.16(11)	O(110)–La(01)–O(1.4)	133.24(12)
O(1.8)–La(01)–O(1.4)	66.84(12)	O(1.6)–La(01)–O(1.4)	86.10(11)
O(1.9)–La(01)–O(1.4)	72.87(11)	O(1.5)–La(01)–O(1.4)	66.84(11)
O(1.3)–La(01)–O(1.4)	61.45(12)	O(1.1)–La(01)–O(1.4)	144.67(10)
O(1.7)–La(01)–O(1.2)	114.32(12)	O(110)–La(01)–O(1.2)	64.07(11)
O(1.8)–La(01)–O(1.2)	176.75(10)	O(1.6)–La(01)–O(1.2)	112.18(11)
O(1.9)–La(01)–O(1.2)	116.80(12)	O(1.5)–La(01)–O(1.2)	63.24(11)
O(1.3)–La(01)–O(1.2)	61.24(12)	O(1.1)–La(01)–O(1.2)	58.08(12)
O(1.4)–La(01)–O(1.2)	111.36(12)		

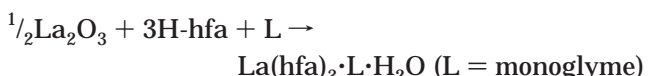
^a Symmetry transformations used to generate equivalent atoms.

X-ray diffraction $\theta/2\theta$ scans were recorded on a computer-interfaced Philips diffractometer using Ni-filtered Cu K α radiation at 20 mA/40 kV.

Results and Discussion

Synthesis. The La(hfa)₃·L adducts have been prepared through a one-pot reaction from lanthanum oxide,

hexafluoroacetylacetone, and polyether in hexane (eq 1)



or



A slight excess of lanthanum oxide favors the isolation of the product since the insoluble excess of La₂O₃ may be easily filtered off. The present syntheses can be efficiently carried out in hexane with good yields, thus avoiding the use of carcinogenic benzene.²⁶ The present synthetic procedure gives rise to nonhygroscopic and water-free adducts **2** and **3**. One H₂O molecule has been found coordinated to the La center in **1** since the small monoglyme polyether cannot efficiently act as partitioning agent. Any attempt to produce water-free monoglyme adducts, even using a 1:2 La:monoglyme ratio in the reaction mixture, proved unsuccessful. Oily products, whose nature prevented any further purification/crystallization, have always been obtained. Note that, at variance with the present La adduct **1**, the homologue Gd complex is water-free due to the smaller ionic radius, which enables the monoglyme to encapsulate the metal ion, thus preventing any water coordination.²⁰

The present adducts are very soluble in common organic solvents such as ethanol, chloroform, acetone, pentane, toluene and slightly soluble in cyclohexane. All the adducts have low melting points and sublime

(26) Malandrino, G.; Licata, R.; Castelli, F.; Fragalà, I. L.; Benelli, C. *Inorg. Chem.* **1995**, *34*, 6223.

Table 8. ^1H and ^{13}C NMR of Adducts **1–3**

complex	^1H NMR			^{13}C NMR			
	COCHCO	H_2O	polyether ^a	COCHCO	COCHCO	CF_3	polyether ^a
1	6.08 (s, 3H)	3.92 (s, 2H) ^b	a 3.54 (s, 6H) b 3.76 (s, 4H)	90.89 (s)	176.97 (q, $^2J = 33\text{Hz}$)	117.59 (q, $^1J = 286\text{ Hz}$)	a 60.49 b 71.68
2	6.08 (s, 3H)		a 3.53 (s, 6H) b, c 3.87 (m, 8H)	90.80 (s)	176.47 (q, $^2J = 34\text{Hz}$)	117.63 (q, $^1J = 286\text{ Hz}$)	a 60.32 b 71.04 c 71.44
3	6.00 (s, 3H)		a 3.36 (s, 6H) b, c 3.75 (m, 8H) d 3.90 (s, 4H)	89.60 (s)	175.72 (q, $^2J = 34\text{Hz}$)	117.79 (q, $^1J = 286\text{ Hz}$)	a 60.38 b, c 70.42, 70.63 d 71.21

^aThe following notation has been used from monoglyme ($\text{CH}_3^{\text{a}}-\text{O}-\text{CH}_2^{\text{b}}$)₂ through triglyme ($\text{CH}_3^{\text{a}}-\text{O}-\text{CH}_2^{\text{b}}-\text{CH}_2^{\text{c}}-\text{O}-\text{CH}_2^{\text{d}}$)₂. ^bThe position of the water peak moves with concentration.

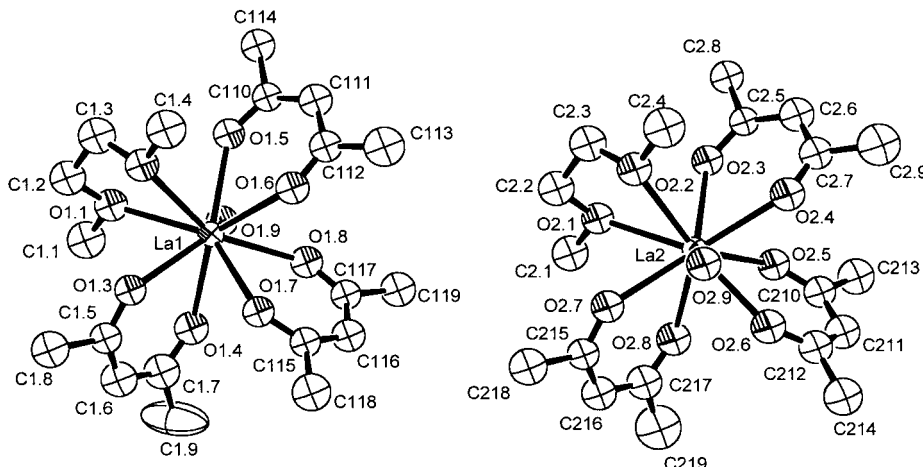


Figure 1. ORTEP drawing of the asymmetric unit of complex $\text{La}(\text{hfa})_3\cdot\text{monoglyme}\cdot\text{H}_2\text{O}$. CF_3 groups have been omitted for clarity.

quantitatively at low temperature under vacuum. They are nonhygroscopic and can be handled in air.

The present syntheses reinforce our earlier assertion on the “general-purpose” features of the one-pot route to the preparation of alkaline-earth ($M = \text{Ba}, \text{Sr}$, and Ca)^{16,17} and rare-earth^{20,26,27} metal adducts. The procedures involve open bench manipulations and yield reproducibly *water-free* products **2** and **3**. Therefore, the polyethers act as hard Lewis bases, which encapsulate the metal ion and favorably compete with H_2O in saturating the coordination sphere around the metal.

Infrared Spectra. The IR spectra of the raw and sublimed $\text{La}(\text{hfa})_3\cdot$ polyether adducts are identical. The absence of any bands around 3600 cm^{-1} in the spectrum of **2** and **3** is indicative of H_2O -free species. By contrast, the weak and sharp bands at 3540 and 3620 cm^{-1} in the spectrum of **1** are associated with water (vide infra) coordination. All the spectra, in addition, show two characteristic peaks around 860 and 1050 cm^{-1} , which may be considered as fingerprints of the glyme coordination to the lanthanum hexafluoroacetylacetone moiety.

NMR Spectra. ^1H and ^{13}C NMR (CDCl_3) data are presented in Table 8. The ^1H NMR spectra always show a singlet ($\delta = 6.0$) associated with the ring proton of the hfa ligand. Different resonances are associated with the polyether framework. Two singlets have been observed in the spectrum of **1** for the methyl ($\delta = 3.54$) and the methylenic ($\delta = 3.76$) groups, an indication of a complete equivalence of the methylenic b protons (see

Table 8 for the notation). In addition, the spectrum of **1** contains a resonance ($\delta = 3.94$) associated with coordinated H_2O . Evaluation of intensities of pertinent resonances points to a 3:1:1 hfa: monoglyme: H_2O ratio. For adduct **2** a single resonance ($\delta = 3.53$) is associated with terminal methyl groups. Bridging methylenic b and c protons are responsible of the multiplet structure centered at $\delta = 3.87$. For the adducts **3**, the methyl groups (a protons) are always observed as a singlet at $\delta = 3.34$. The b and c protons are observed as a multiplet centered at $\delta = 3.75$. The protons d are associated with a singlet at $\delta = 3.90$.

The ^{13}C NMR (CDCl_3) spectra (Table 8) can be assigned using comparative arguments with data from related alkaline-earth complexes.^{11,17} Thus, resonances associated with the coordinated hfa ligands consist, in all cases, of singlets ($\delta \approx 90$) for the CH group, quartets ($\delta \approx 117$) for the CF_3 groups, and quartets ($\delta \approx 176$) for the CO groups. The quartets are due to first order (CF_3 ; $^1J = 286\text{ Hz}$) and second order (CO ; $^2J = 34\text{ Hz}$) coupling with the CF_3 fluorine atoms. Coordinated glymes give signals at $\delta = 60.49$ (s, OCH_3 , a) and $\delta = 71.68$ (s, OCH_2 , b) in the spectrum of **1**. In the case of **2**, the diglyme signals are observed at $\delta = 60.32$ (s, OCH_3 , a), $\delta = 71.04$ (s, OCH_2 , b), and $\delta = 71.44$ (s, OCH_2 , c). For the adduct **3**, the triglyme signals are observed at $\delta = 60.38$ (s, OCH_3 , a), 70.42 (s, OCH_2 , b), 70.63 (s, OCH_2 , c), and 71.21 (s, OCH_2 , d).

X-ray Single-Crystal Structures of $\text{La}(\text{hfa})_3\cdot\text{Monoglyme}\cdot\text{H}_2\text{O}$, $\text{La}(\text{hfa})_3\cdot\text{Diglyme}$ and $\text{La}(\text{hfa})_3\cdot\text{Triglyme}$. The ORTEP drawings of $\text{La}(\text{hfa})_3\cdot\text{monoglyme}\cdot\text{H}_2\text{O}$ and $\text{La}(\text{hfa})_3\cdot\text{diglyme}$ are reported in Figures 1 and 2, respectively. Positional parameters and se-

(27) Malandrino, G.; Fragalà, I. L.; Aime, S.; Dastrù, W.; Gobetto, R.; Benelli, C. *J. Chem. Soc., Dalton Trans.* **1998**, 1509.

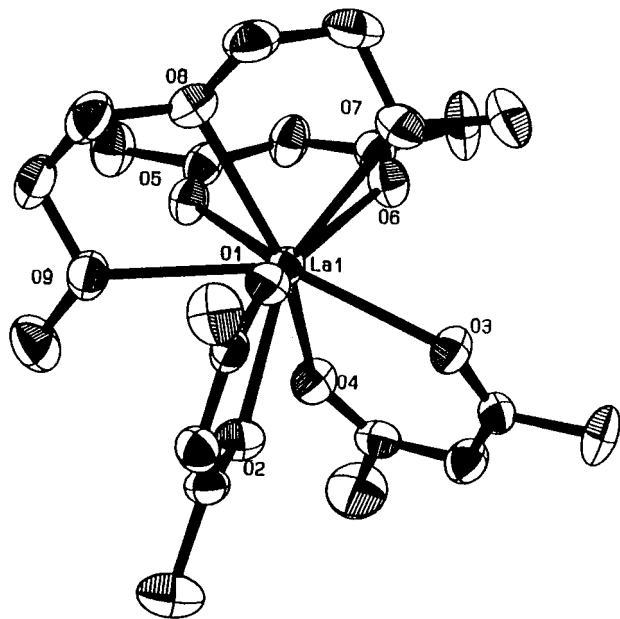


Figure 2. ORTEP drawing of the crystal structure of $\text{La}(\text{hfa})_3\cdot\text{diglyme}$. CF_3 groups have been omitted for clarity.

lected bond distances and angles of **1** and **2** are compiled in Tables 2 and 3, and 4 and 5, respectively. The crystal structures of **1** and **2** consist of asymmetric units containing two and one molecules, respectively. The structures of **1** and **2**, some details of **2** have previously been communicated,²⁶ consist of mononuclear 9-coordinated arrays with square antiprismatic geometries. The coordination sphere of **1** involves the six oxygens of the $(\text{hfa})_3$ cluster, the two oxygens of the monoglyme ligand, and the H_2O ligand capping one face.²⁸ The oxygen atoms of the three hfa (six oxygens) and of the diglyme (three oxygens) ligands are all involved in the coordination with the ninth oxygen atom (O8) (Figure 2) capping one of the square faces.

The average $\text{La}-\text{O}(\text{hfa})$ lengths of **1** (2.512 and 2.516 Å in the two molecules) are shorter than found in **2** (2.533 Å) and longer (vide infra) than in **3** (2.50 Å), while the average $\text{La}-\text{O}(\text{monoglyme})$ distances (2.613 Å) are slightly larger than in **2** (2.547 Å) and slightly smaller than in **3** (2.68 Å). The average $\text{La}-\text{O}(\text{glyme})$ bond distances (2.613 Å in **1** and 2.547 Å in **2**) are considerably shorter than found in the similarly 9-coordinated $\text{La}(\text{tmhd})_3\cdot\text{tetraglyme}$ ¹ (2.706–2.781 Å). This is indicative of a stronger coordination involving the La center and the polyether donor atoms. Finally, note that the structure of the $\text{La}(\text{hfa})_3\cdot\text{diglyme}$ resembles that of the gadolinium analogue, even though a larger difference (0.150 Å) is observed between the average $\text{Gd}-\text{O}(\text{diglyme})$ and the average $\text{Gd}-\text{O}(\text{hfa})$ distances, compared to 0.014 Å in the La analogue. This observation may be related to the larger ionic radius of the lanthanum(III) vs gadolinium(III) ion.

The ORTEP drawing of $\text{La}(\text{hfa})_3\cdot\text{triglyme}$ is shown in Figure 3. Positional parameters and selected bond distances and angles are reported in Tables 6 and 7, respectively. The crystal structure of **3** consists of a very complex asymmetric unit with four rather similar molecules (Figure 4), each containing a 10-coordinated

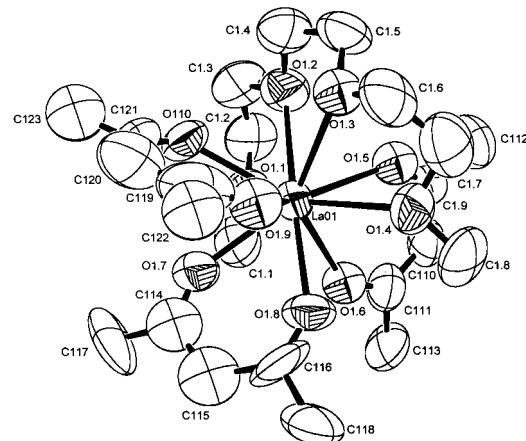


Figure 3. ORTEP drawing of one of the four molecules present in the asymmetric unit of $\text{La}(\text{hfa})_3\cdot\text{triglyme}$. CF_3 groups have been omitted for clarity.

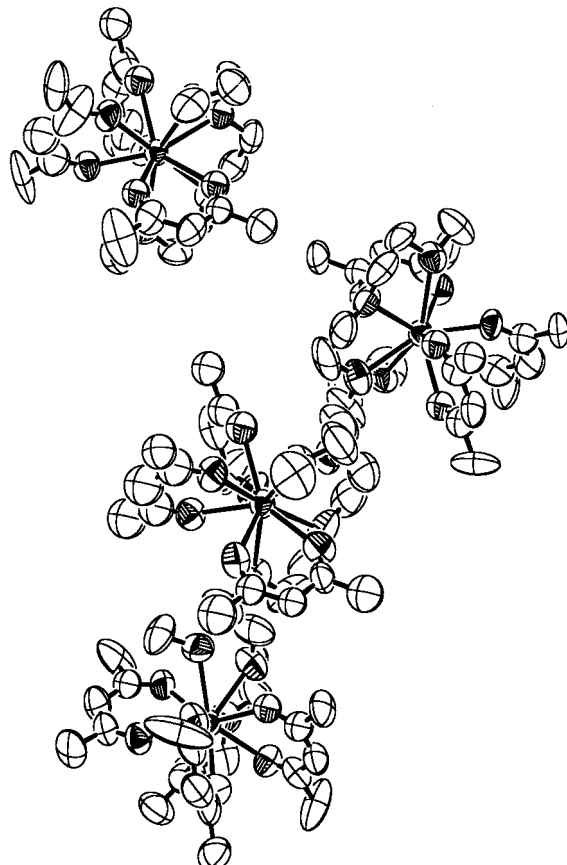


Figure 4. ORTEP drawing of the asymmetric unit of complex $\text{La}(\text{hfa})_3\cdot\text{triglyme}$. CF_3 groups have been omitted for clarity.

lanthanum(III) ion. The coordination sphere involves, in addition to the six oxygen atoms of the $(\text{hfa})_3$ cluster, the four oxygen atoms of the triglyme ligand, thus defining a higher distorted polyhedron than expected for the 10 coordination. This coordination appears to be at the limit of acceptability, and a longer polyether such as tetraglyme coordinates only four of the five oxygens.²⁷ The 10-coordination is, in fact, rather uncommon and has been observed only in few cases.²⁹ The average $\text{La}-\text{O}(\text{hfa})$ lengths are almost identical in the

(28) Sinha, S. P., *Struct. Bonding (Berlin)* **1976**, 25, 69.

(29) Rogers, R. D.; Rollins, A. N.; Etzenhouser R. D.; Voss, E. J.; Bauer, C. B. *Inorg. Chem.* **1993**, 32, 3451.

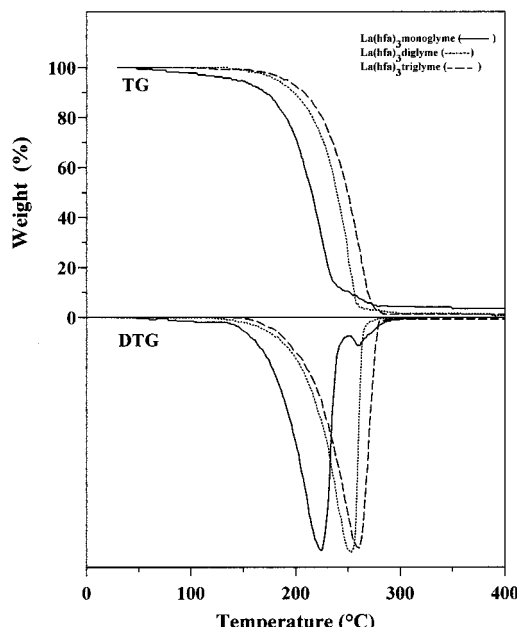


Figure 5. TG–DTG curves of adducts **1–3**.

four molecules of the asymmetric unit and range from 2.491 to 2.509 Å. Similarly, the average La–O(triglyme) bond distances lie in a narrow 2.679–2.688 Å range. Within the asymmetric units, the four molecules are well-separated with no evidence of any kind of interaction. The shortest intermolecular distance is 2.38 Å between two carbon atoms belonging to methyl groups of triglyme molecules; all the other intermolecular contacts are longer than 2.5 Å.

Mass Transport Properties. Thermal behaviors of the raw adducts $\text{La}(\text{hfa})_3 \cdot \text{L}$ have been studied by atmospheric pressure thermal gravimetric analysis (TG), differential thermal gravimetric analysis (DTG), and atmospheric pressure TG vaporization rate experiments.³⁰ The TG curves of **1–3** are reported in Figure 5. The monoglyme adduct shows a 89% weight loss in the 53–251 °C range and a 7% loss in the 251–341 °C range with 4% residue left at 350 °C. Singular sublimation steps are observed for the diglyme and triglyme adducts in the temperature range of 115–295 °C (residue = 2% to 300 °C) and 143–296 °C (residue = 1% to 300 °C), respectively. TGA atmospheric pressure vaporization rates of adducts **1–3** are compared to data of $\text{La}(\text{tmhd})_3 \cdot \text{H}_2\text{O}$ in Figure 6. It becomes evident that all the adducts are more volatile than the “first-generation” $\text{La}(\text{tmhd})_3 \cdot \text{H}_2\text{O}$ precursor, and in particular, adducts **1**, **2** and **3** vaporize ca. 29, 12, and 7 times more rapidly than $\text{La}(\text{tmhd})_3 \cdot \text{H}_2\text{O}$, respectively. Note that on lengthening the polyether chain there is a corresponding decrease in the volatility of the present adducts. Earlier data have shown that the $\text{La}(\text{hfa})_3 \cdot$ tetraglyme²⁷ vaporizes ca. 3 times more rapidly than the first generation precursor, $\text{La}(\text{tmhd})_3 \cdot \text{H}_2\text{O}$. There is, therefore, evidence of an intriguing interplay between the polyether chain length and the lanthanum ionic radius in determining the volatility of these adducts. A small polyether, such as the monoglyme, is adducted to form a very volatile lanthanum precursor which, unfortunately, coordinates

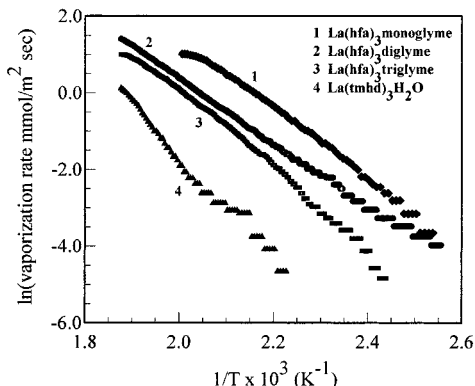


Figure 6. Atmospheric-pressure TG vaporization rate data of adducts **1–3** compared to $\text{La}(\text{tmhd})_3 \cdot \text{H}_2\text{O}$ as a function of temperature.

Table 9. Major Peaks in the Mass Spectra of Adducts 2 and 3^a

assignment	M = $\text{La}(\text{hfa})_3 \cdot \text{diglyme}$	M = $\text{La}(\text{hfa})_3 \cdot \text{triglyme}$
$[\text{M} - \text{hfa}]^+$	687 (100%)	731 (100%)
$[\text{M} - \text{hfa} - \text{L}]^+$	553 (28%)	553 (<5%)
$[\text{M} - 2\text{hfa} + \text{F}]^+$	499 (24%)	543 (9%)
$[\text{M} - 2\text{hfa} - \text{L} + \text{F}]^+$	365 (11%)	365 (<5%)
$[\text{M} - 2\text{hfa} - \text{L}]^+$	346 (<5%)	346 (<3%)
$[\text{M} - 3\text{hfa} + 2\text{F}]^+$	311 (<5%)	355 (7%)

^a For the assignment of adduct **1** see the scheme in Figure 7.

one H_2O molecule. The diglyme and triglyme polyethers form adducts with excellent properties in terms of thermal stability and volatility. The longer tetraglyme, finally, with its five oxygen atoms, exceeds the acceptor capabilities of the La(III) ion and, in fact, only four of the five oxygens coordinate.²⁷

To our knowledge, the present “second-generation” adducts represent the first examples of thermally stable lanthanum β -diketonate polyether adducts which sublime intact, even under atmospheric pressure. The earlier reported $\text{La}(\text{tmhd})_3 \cdot$ tetraglyme decomposes, in fact, upon sublimation in *vacuo* to yield the unadducted tmhd complex.¹

Mass Spectra. The FAB spectra of the adducts **1–3** are reported in Table 9. No molecular ion peaks or peaks at higher mass have been observed for **2** and **3**, whose spectra show fragment peaks due to the loss of both the H-hfa and polyether ligands. In addition, there is evidence of the characteristic fluorine transfer process, already observed in the spectra of the analogous alkaline-earth^{12,16,17} and gadolinium adducts.²⁰ The major peak of **2** and **3** corresponds to the ion $[\text{La}(\text{hfa})_2 \cdot \text{L}]^+$. At lower mass, the more abundant peaks correspond to the fragments $[\text{La}(\text{hfa}) \cdot \text{L} + \text{F}]^+$, $[\text{La} \cdot \text{L} + 2\text{F}]^+$, $[\text{La}(\text{hfa})_2]^+$, $[\text{La}(\text{hfa}) + \text{F}]^+$.

The spectrum of the monoglyme adduct shows higher mass peaks than the monomeric species. Gas-phase aggregation processes due to the FAB technique can be ruled out since there is not any similar evidence in FAB spectra of either **2** and **3** or a large number of analogous lanthanide adducts.^{20,31} Rather, the distance (2.72 Å) between a fluorine and a hydrogen atom of the two molecules observed in the X-ray crystal structure (vide infra) compares well with the sum of the van der Waals

(30) Experiments were performed with a temperature ramp up of 5 °C/min under N_2 and with a 4 mm alumina sample pan.

(31) Malandrino, G.; Fragalà, I. L. Unpublished results on europium and neodium adducts.

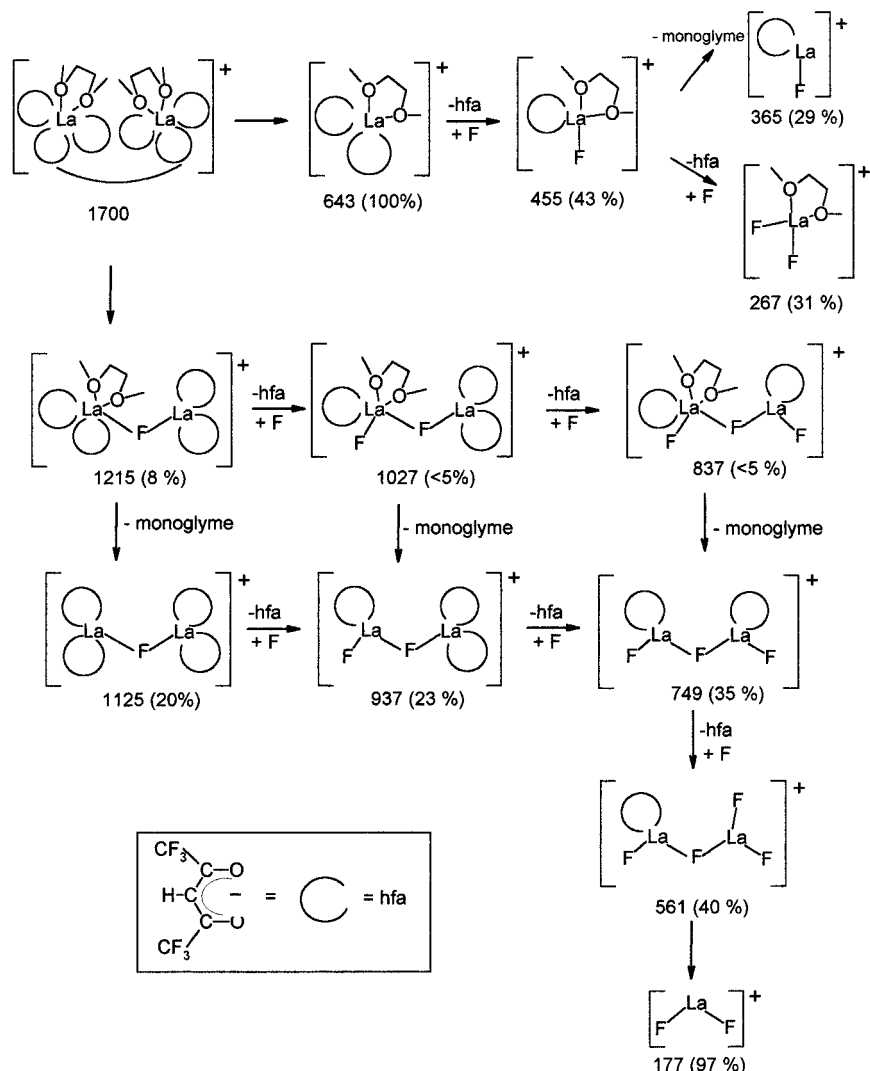


Figure 7. A hypothetical assignment of the FAB mass spectrum of the adduct $\text{La}(\text{hfa})_3 \cdot \text{monoglyme} \cdot \text{H}_2\text{O}$.

radii³² and may stabilize a dimeric unit in the gas phase. In accordance, the fragmentation pattern observed in the FAB spectrum of **1** seems consistent with a gas-phase dimer (Figure 7).

MOCVD Depositions. The diglyme adduct has been successfully applied to the atmospheric-pressure deposition of LaF_3 films and to the low-pressure deposition of LaAlO_3 thin films.²⁵ The X-ray diffraction scan of the atmospheric-pressure deposited LaF_3 film on Si (111) substrate is reported in Figure 8. Wavelength dispersive X-ray analyses are indicative of minor (<3%) amounts of carbon contamination. Note that the fluorinating agent is supplied from the source material itself. A typical X-ray diffraction pattern of LaAlO_3 thin films deposited on YSZ substrate is reported in Figure 9. Reflections point unequivocally to a dominant (111) orientation of polycrystalline films and, accordingly, a narrow 0.75° half-maximum full-width has been measured in the (111) rocking curve.

Conclusions

The present one-pot synthetic strategy has proven to be an efficient route for preparation of thermally stable and volatile lanthanum and gadolinium second-generation adducts from commercially available products. To

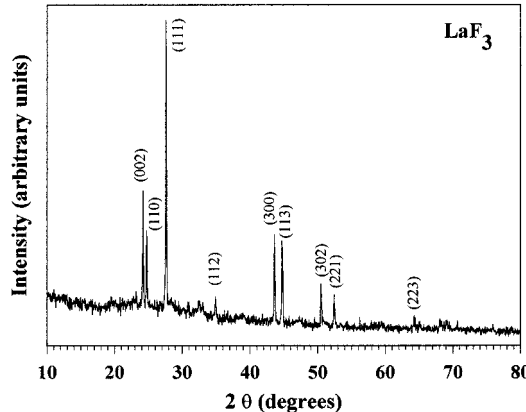


Figure 8. X-ray diffraction pattern of an MOCVD grown LaF_3 film on (111) Si substrate using the $\text{La}(\text{hfa})_3 \cdot \text{diglyme}$ as single source precursor.

our knowledge, adducts **1–3** represent the first examples of thermally stable lanthanum β -diketonate polyether adducts which can be contrasted with the $\text{La}(\text{tmhd})_3 \cdot \text{tetraglyme}$, which decomposes upon sublima-

(32) Huheey, J. E.; Keiter, E. A.; Keiter, R. L. *Inorganic Chemistry: Principles of Structure and Reactivity*, 4th ed.; Harper Collins College Publishers: New York, 1993.

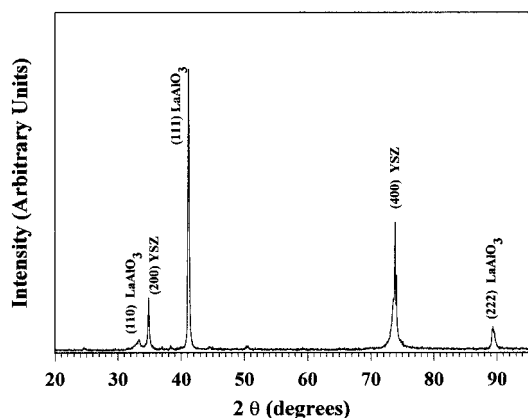


Figure 9. X-ray diffraction pattern of an in situ MOCVD-grown LaAlO_3 film on YSZ (100) substrate using the La(hfa)_3 ·diglyme and the Al(acac)_3 as precursors.

tion to yield the unadducted tmhd complex.¹ Even more interestingly, thermogravimetric and vaporization rate experiments indicate that they can be used in atmospheric-pressure MOCVD deposition at temperatures lower than 200 °C with better mass transport properties and thermal behavior than conventional rare-earth metal CVD precursors.

In addition, their low melting points allow their use as thermally stable precursors in the liquid phase, hence under constant vaporization and mass transport rates. Finally, adducts **1–3** act as liquid solvents for a large variety of relevant precursor complexes, thus providing liquid single-sources which simultaneously deliver all the metal components in the required stoichiometry.²⁵

Their vapor-phase transport characteristics at low and atmospheric pressure make them attractive candidates not only for laboratory MOCVD processes but also for industrial application.

Acknowledgment. The authors thank the Consiglio Nazionale delle Ricerche (CNR, Rome, Progetto Finalizzato Nazionale Materiali Avanzati II) for financial support.

Supporting Information Available: A complete list of crystal structure analysis, atom positions, thermal parameters, bond distances and bond angles of adducts **1–3**, and ORTEP drawings of the second, third and fourth molecules of the asymmetric unit of **3** (26 pages). Ordering information is given on any current masthead page.

CM980172J